

Detectability of Hypometabolic Regions in Mild Alzheimer Disease: Function of Time after the Injection of 2-[Fluorine 18]-Fluoro-2-Deoxy-D-Glucose

Setsu Sakamoto, Kazunari Ishii, Kayo Hosaka, Tetsuya Mori, Masahiro Sasaki, and Etsuro Mori

BACKGROUND AND PURPOSE: 2-[Fluorine 18]-fluoro-2-deoxy-D-glucose (FDG) positron emission tomography (PET) has played an important role in detecting hypometabolic regions in the brains of patients with dementia. To our knowledge, the optimal imaging time for dementia has not been investigated. The aim of this study was to evaluate the sensitivity of the early scanning (ES) compared with late scanning (LS) for demonstrating decreased regional glucose metabolism in patients with Alzheimer disease (AD).

METHODS: Twenty patients with mild AD (mean age \pm standard deviation, 64.8 ± 5.2 years) and 20 age- and sex-matched healthy volunteers (age, 65.9 ± 4.5 years) were underwent FDG PET. Their cerebral glucose metabolic images were obtained on ES at 30–42 minutes and LS at 60–72 minutes after the administration of FDG 185–346 MBq. We compared regional cerebral metabolic images in a voxel-by-voxel analysis with statistical parametric mapping between patients with AD and control subjects and evaluated the difference in the hypometabolic regions between the two scans.

RESULTS: In the AD-to-healthy comparison, LS at the $P < .001$ level of significance showed more extensive and significant hypometabolic areas than did ES.

CONCLUSION: These results indicate that LS is superior to ES in detecting hypometabolic regions in patients with AD. For patients with AD, emission scanning soon after the administration of FDG is probably not advised.

2-[Fluorine 18]-fluoro-2-deoxy-D-glucose (FDG) positron emission tomography (PET) plays an important role in the diagnosis of dementia by depicting hypometabolic regions. Kumar et al (1) found no significant differences in the regional cerebral metabolic ratio for glucose between early scanning (ES) starting at 30 minutes and late scanning (LS) starting at 45 minutes after the administration of 2-[Fluorine 18]-fluoro-2-deoxy-D-glucose (FDG) in patients with Alzheimer disease (AD) compared with healthy control subjects. Because of amnesia, inattention or impatience, patients with AD often cannot keep still during the long period required for data acquisition.

Movements during positron emission tomography (PET) cause motion artifacts and poor image quality. One solution is to shorten the total examination time. If ES has sensitivity similar to that of ordinary scanning for hypometabolic regions, the examination time can be reduced. Contrast-enhanced transmission scanning has successfully shortened the examination period in accordance with the development of PET scanners, though the best time for emission scanning to detect regional metabolic changes in AD and in healthy subjects has not been adequately evaluated. The optimal FDG PET imaging time for evaluating cancer has been debated, though the images are known to demonstrate increased activity at later rather than earlier time points in relation to tumor grade. FDG PET demonstrates regional glucose metabolic reduction in dementia; however, to our knowledge, investigations of its optimal imaging time have not been conducted. If ES has sensitivity for hypometabolic regions similar to that of an ordinary scanning or LS, the total examination time can be reduced.

Because Kumar et al (1) performed their analysis with multiple regions of interest (ROIs), some re-

Received May 25, 2004; accepted after revision August 16.

From the Departments of Radiology and Nuclear Medicine, Hyogo Brain and Heart Center, Himeji (S.S., K.I., K.H., T.M., M.S., E.M.); the Division of Image-Based Medicine, Institute of Biomedical Research and Innovation, Kobe (S.S.); the Department of Radiology, Kobe University School of Medicine (K.H.); and the PET Center, Himeji Central Hospital, Hyogo (M.S.), Japan.

Address reprint request to Dr Kazunari Ishii, Department of Radiology and Nuclear Medicine, Hyogo Brain and Heart Center, 520 Saisho-Ko, Himeji, Hyogo 670-0981, Japan.

gions where ROIs were not placed might not have been adequately analyzed. On the contrary, voxel-by-voxel comparison has a more appropriate anatomic standardization technique and has been well used in group comparisons of PET images. We analyzed ES and LS FDG PET images by using voxel-by-voxel analysis and statistical parametric mapping (SPM) and evaluated which scanning time was appropriate for demonstrating decreased regional glucose metabolism in patients with AD. We also evaluated the diagnostic performance of ES and LS in the group with AD, comparing with individual patient's ES and LS images.

Methods

Subjects

We enrolled patients with mild AD (13 women and seven men; mean age \pm standard deviation, 64.8 ± 5.2 years), and 20 age- and sex-matched healthy volunteers (14 women and six men; age, 65.9 ± 4.5 years). Patients with AD were selected from those admitted to our hospital for examination and fulfilled currently accepted criteria for diagnosis of AD set by the National Institute of Neurologic Disease and Stroke/Alzheimer Disease and Related Disorders Association. Patients had no evidence of focal brain lesions except for brain atrophy or age-related hyperintensity on T2-weighted images. All patients with AD had scores of over 20 on the Mini-Mental State Examination, with a mean score of 23.6 ± 2.3 . The control subjects had no clinical evidence of cognitive deficits or neurologic disease and were taking no short- or long-term medications at the time of scanning. Their MR images showed no abnormal findings. Before the examination, all participants provided written informed consent. All procedures followed the clinical study guidelines of our institute, and were approved by the Institutional Review Board.

PET Procedure

Before PET scanning, both patients and control subjects underwent MR imaging to confirm that they had no abnormal conditions. Detailed PET and MR imaging procedures are described elsewhere (2). Briefly, PET was performed with a PET scanner (Headtome IV; Shimadzu Corp., Kyoto, Japan) that yielded a transverse resolution of 4.5 mm full width at half maximum (3). The section interval was 6.5 mm with the z-motion mode. A transmission scan was obtained by using a $^{68}\text{Ga}/^{68}\text{Ge}$ pin source for absorption correction after each subject was positioned. PET studies were performed under conditions of rest with the patients' eyes closed and ears unplugged. All subjects had fasted for at least 4 hours before PET scanning. Static sequences were started at 30 and 60 minutes after the injection of FDG 169–346 MBq, and emission data were collected for 12 minutes each. Both static sequences were used to obtain qualitative images.

Data Analysis

PET and MR image datasets were directly transmitted to a workstation (Indigo2 Extreme; Silicon Graphics, Mountain View, CA) from the PET and MR imaging units and analyzed by using image-analyzing software (Dr. View, version 5.3; Asahikasei Jyoho System, Tokyo, Japan). To delineate the differences between ES and LS, we prepared two sets of PET data. For the ES images, we used the static images obtained 30 minutes after injection, and for the LS images, we used the static images obtained 60 minutes after injection. All the datasets were then converted to binary format and transferred to a computer (Logitech Corp., Tokyo, Japan) running Windows

software (Microsoft Corp., Redmond, WA) for statistical analysis.

Statistical Analysis

We used Neurostat software (University of Michigan, Ann Arbor, MI) for anatomic standardization of PET images, as brain atrophy is sometimes seen in patients. In a previous study (4), we found that Neurostat was more suitable than Statistical Parametric Mapping 99 (SPM99; the Wellcome Department of Neurology, London, UK) for anatomic standardization of atrophied brains. The image sets were transformed to a standard stereotactic space by using the part of the program Neurostat that generates standardized, three-dimensional, stereotactic surface projections (3D-SSP) datasets for individual subjects (5). Then, statistical processing was performed with SPM99 software to evaluate the regional differences. Calculations and image matrix manipulations were performed in Matlab (version 5.3; Mathworks Inc., Natick, MA) and spatially smoothed by using an isotropic gaussian filter to compensate for intersubject gyral variability and to reduce high-frequency noise, with a resolution of 12 mm full width at half maximum. The stereotactically normalized FDG PET images were adjusted for individual differences in global metabolism by using covariance analysis. The algorithm scaled all images to a global mean glucose metabolic rate of 5.0 mg/100 g/minute. Finally, comparative analysis between the groups was performed on a voxel-by-voxel basis for all voxels common to all subjects (6). The sensitivity for detecting hypometabolism at each time window (ES vs LS) was evaluated by counting the number of voxels, which showed a significant area of reduced metabolism in the AD group. A paired *t* test (SPM 99) was also performed between ES and LS in patients with AD and in control subjects. The level of significance was set at $P < .001$, uncorrected.

Individual Z-score maps for ES and for LS were generated by using iSSP software (Nikon Medipysics Corp., Nishinomiya, Japan), which consisted of 3D SSP programs and which were specifically designed to support clinical diagnoses. For this, we used the database consisting of ES and LS images in the control group. To evaluate the diagnostic performance of ES and LS in the AD group, the Z-score maps were compared by means of visual inspection of individual ES and LS images. We visually compared the extent of the pixels with a Z score of more than 2.0 and also the maximum value of Z scores in the parietotemporal and posterior cingulate area between the each Z-score map for ES and LS in patients with AD. One reader (KI) interpreted both the extent and the height of the Z-score, as follows: For extent, $ES > LS$ indicated that the extent of pixels with a Z score of more than 2.0 was larger with ES than with LS. $ES = LS$ indicated that the extent of pixels with a Z score of more than 2.0 was almost equal with ES and with LS. $ES < LS$ indicated that the extent of pixels with a Z score of more than 2.0 was smaller with ES than with LS. Regarding height, $ES > LS$ meant that the maximum Z score in the parietotemporal and posterior cingulate area was larger with ES than with LS. $ES = LS$ meant that the maximum Z score in the parietotemporal and posterior cingulate area was almost equal with ES and with LS. $ES < LS$ meant that the maximum Z score in the parietotemporal and posterior cingulate area was smaller with ES than with LS.

The diagnostic performance, ie, whether each Z-score map from ES and LS had an AD metabolic reduction pattern (temporoparietal and/or posterior cingulate reduction pattern), was estimated for each patient with AD.

Results

ES showed that posterior cingulate metabolism was significantly reduced in the AD group compared with the control group, whereas LS showed both the posterior cingulate and right temporal metabolism signif-

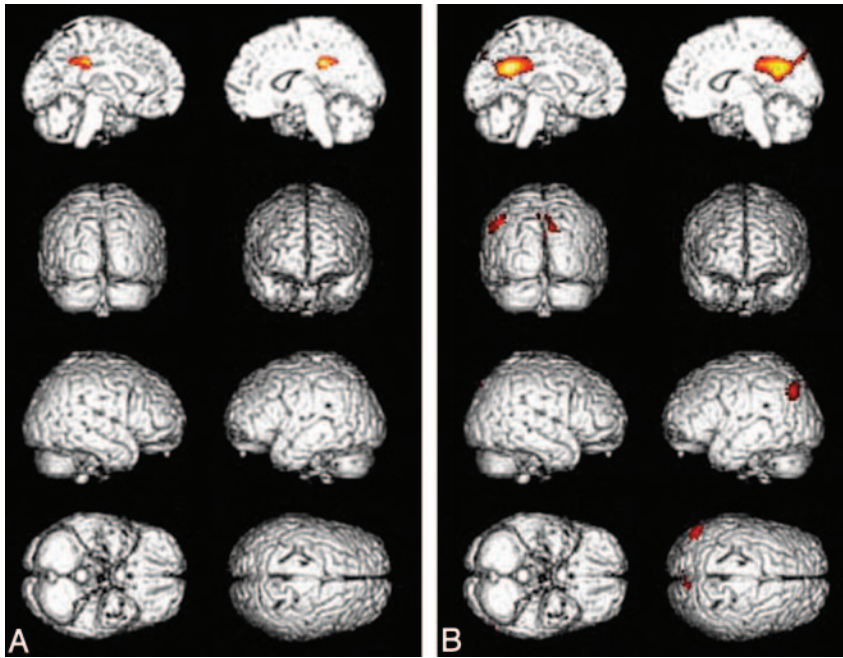


FIG 1. Comparison of patients with AD and healthy control subjects by using SPMs. *Highlighted areas* indicate regions with significantly decreased FDG uptake ($P < .001$).

A, ES at 30 minutes after FDG injection.
B, LS at 60 minutes after FDG injection.

TABLE 1: Regions of relative hypometabolism in patients with AD versus control subjects

Group and Brain Region	<i>x</i>	<i>y</i>	<i>z</i>	<i>t</i> Value	k_E^*
LS					
L posterior cingulate gyrus	9	-54	23	5.37	1598
R angular gyrus	-54	-70	36	3.93	202
ES, L posterior cingulate gyrus	5	-38	34	4.19	195

Note.—Threshold is $P < .001$, uncorrected.

* k_E = No. of extent voxels.

icantly reduced in the AD group compared with the control group. LS showed 1800 voxels of significant hypometabolic areas in patients with AD compared with control subjects, whereas ES showed 195 voxels of significant hypometabolic areas in the whole brain at the threshold of $P = .001$ (Fig 1, Table 1). The peak height of the *t* value was 5.37 for LS and 4.19 for ES in the left posterior cingulate gyrus.

We observed no significantly decreased or increased metabolic area between ES and LS images in patients with AD. However, metabolism in precuneus, temporal, frontal and parietal areas was significantly reduced on ES images compared with LS images in the control group at the threshold of $P = .001$ (Fig 2, Table 2).

Table 3 shows the results of visual inspection. In 14 patients, the extent of reduced metabolic area was larger on LS than on ES, and the peak Z score from the LS image was higher than that of the ES image. The Z-score maps from both ES and LS demonstrated an AD reduction pattern (except in patient 3), but the AD pattern was more clearly demonstrated on the Z-score maps from LS than on those from ES because of the larger extent and height of the pixels of Z scores.

Figure 3 shows the Z-score maps at ES and LS in a patient with AD (patient 9).

Discussion

We used voxel-based statistical analysis to compare scans starting at 30 and at 60 minutes after the injection of FDG and evaluated differences in the rate of detecting hypometabolic regions in AD between these two time windows. We found that the 60-minute scan showed larger and more significant abnormalities in AD than in controls. We believe that our report is the first to evaluate the appropriate time required for emission scanning to detect regional metabolic changes in AD.

Kumar et al (1) showed that, under stable experimental conditions, potential errors in rate constants, which are functions of time, do not significantly influence the measurement of the cerebral metabolic rate for glucose, and they concluded that FDG PET can be reliably performed 30 minutes after intravenous injection. However, their analysis was based on ROIs in limited areas. Therefore, they included no evidence allowing for the metabolic differences underlying the two sets of images starting at 30 and 45 minutes after the administration of FDG. Our study was based on voxel-by-voxel analysis and revealed differences in the detectability of hypometabolism in the same patient groups. The number of voxels showing significantly decreased metabolism in the AD group compared with control group during LS was 9.0 times larger than the number detected with ES. The areas with significantly reduced metabolism in the posterior cingulate gyrus were more widely spread with the LS data than with the ES data.

The reasons for the differences are unclear. One explanation is the regional difference in lumped constant and kinetic rate constants among every brain region. Rate constants change not only over time but also in gray matter and white matter, and the effect of tissue heterogeneity on the calculation of rate constants decrease with time (7). In healthy subjects, LS

FIG 2. Areas of low regional cerebral FDG uptake shown on SPMs in healthy subjects at ES (30 minutes) versus LS (60 minutes).

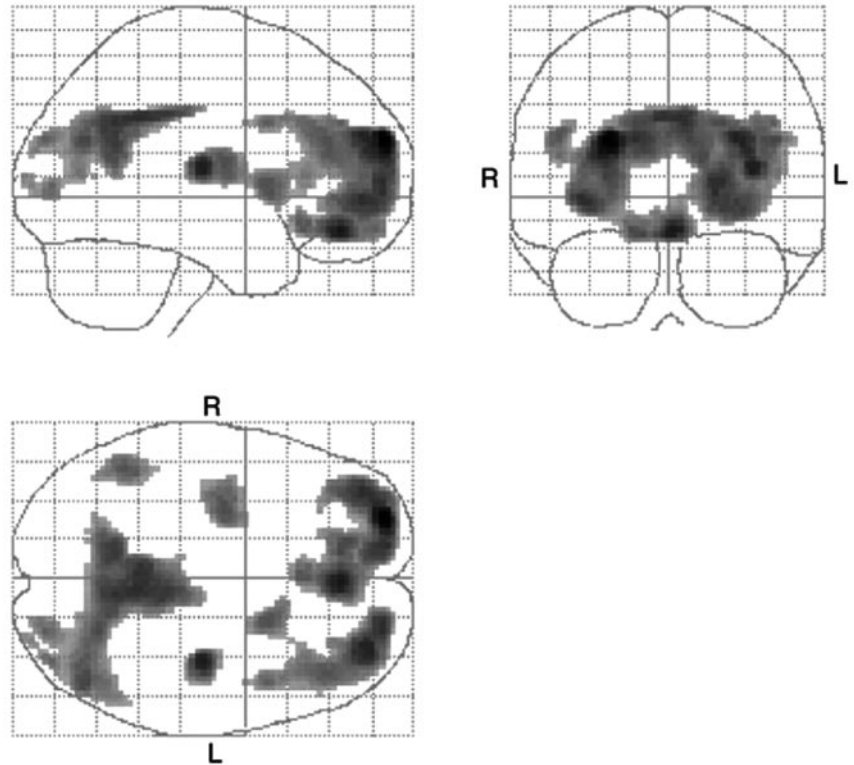


TABLE 2: Regions of relative hypometabolism on ES versus LS in control subjects

Brain region	x	y	z	t Value	k_E^*
R superior frontal gyrus	-27	59	25	6.55	1888
L superior temporal gyrus	36	-18	11	5.50	165
L superior frontal gyrus	29	52	25	5.35	1643
L precuneus	5	-47	34	5.18	2022
R supramarginal gyrus	-47	-52	27	4.54	172

Note.—Threshold is $P < .001$, uncorrected.
 * k_E = No. of extent voxels.

showed larger FDG uptake in the bilateral posterior cingulate gyri, parietal and frontal association cortices, and subcallosal cortices than that shown on ES. In addition, relatively large FDG uptake was observed in the frontal bases, cerebellar hemisphere, and vermis on ES than on LS, as demonstrated in voxel-by-voxel analysis (8). In normal brain, these differences between the two sets of scans may be related to regional differences of rate constants, such as K_1 , which indicates FDG transportation from plasma to tissue, and k_3 , which indicates phosphorylation of FDG. In AD, glucose metabolism is altered by neurodegeneration (9, 10), and k_3 is most affected constant in the parietotemporal region. In patients with AD, altered phosphorylation in the affected regions may cause differences in FDG uptake that are larger than those of control subjects in the late period after intravenous injection. As the plasma concentration decreases, k_3 may theoretically have a greater influence on uptake at a later time point, and this may explain the greater reduction of metabolism in patients with AD if scanning was performed later rather

TABLE 3: Results of visual inspection of Z-score maps in patients with AD

Patient	Age (y)	MMSE Score*	Extent†	Height†	AD Pattern‡	
					ES	LS
1	56	20	ES < LS	ES < LS	Yes	Yes
2	70	20	ES < LS	ES = LS	Yes	Yes
3	63	21	ES = LS	ES < LS	No	No
4	68	21	ES = LS	ES = LS	Yes	Yes
5	66	22	ES = LS	ES = LS	Yes	Yes
6	68	22	ES < LS	ES < LS	Yes	Yes
7	74	22	ES < LS	ES < LS	Yes	Yes
8	63	23	ES < LS	ES < LS	Yes	Yes
9	67	23	ES < LS	ES < LS	Yes	Yes
10	69	23	ES < LS	ES = LS	Yes	Yes
11	70	23	ES = LS	ES = LS	Yes	Yes
12	62	24	ES < LS	ES < LS	Yes	Yes
13	64	24	ES < LS	ES = LS	Yes	Yes
14	65	25	ES < LS	ES < LS	Yes	Yes
15	67	25	ES = LS	ES < LS	Yes	Yes
16	56	26	ES < LS	ES < LS	Yes	Yes
17	64	26	ES < LS	ES = LS	Yes	Yes
18	53	27	ES < LS	ES < LS	Yes	Yes
19	63	27	ES < LS	ES < LS	Yes	Yes
20	68	27	ES = LS	ES = LS	Yes	Yes

* MMSE = Mini-Mental State Examination.
 † ES < LS indicates that the extent of the Z score more than 2.0 or that the maximum Z score in the parietotemporal and posterior cingulate area was larger with ES than with LS; ES = LS, the extent of the Z score or the maximum Z score was approximately equal; and ES > LS, the extent of the Z score or the maximum Z score was smaller with ES than with LS.
 ‡ Yes = temporoparietal and/or posterior cingulate reduction pattern existed; No = pattern did not exist.

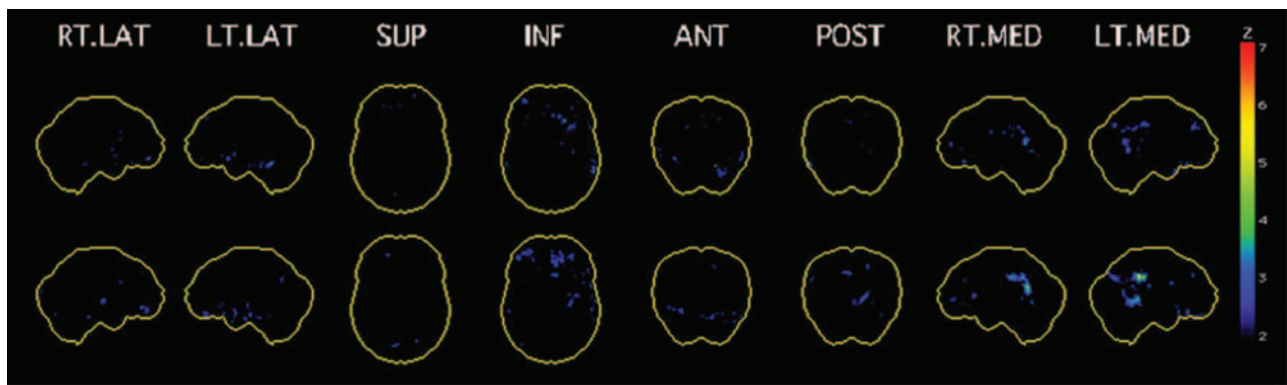


FIG 3. Z-score images of a 67-year-old woman AD (Mini-Mental State Examination score of 23, Alzheimer's Disease Assessment Scale score of 20) at ES (*top*) and at LS (*bottom*). Distribution of areas of significantly decreased FDG uptake are larger and the height of the Z score is larger on the LS image than on the ES image, especially in the posterior cingulate gyrus and precuneus. Views: RT.LAT = right lateral, LT.LAT = left lateral, SUP = superior, INF = inferior, ANT = anterior, POST = posterior, RT.MED = right medial, LT.MED = left medial.

than earlier after injection. These factors were mainly due to regional differences in the control group and not regional difference in the AD group. The reason may be because the uptake of FDG in the posterior cingulate gyrus and parietal association cortices in the AD brain does not gradually increase in a time-dependent manner, as it does in the control brain.

Nowadays, most scanners can be used to perform postinjection transmission scanning, and the duration of brain scanning is as short as 5 minutes with some PET scanners (11). Even with use of this postinjection transmission scanning technique, the best time for emission scanning should be evaluated. Our data indicated LS is superior to ES for detecting hypometabolic regions in patients with AD. This finding does not necessarily mean that scanning at an earlier times after injection leads to the overlooking of hypometabolic regions in patients with AD. We must be aware that shortening of the examination time may reduce the sensitivity of detecting AD with FDG PET. In addition, with postinjection transmission and emission scanning, starting the study soon after the injection of FDG is not preferred, and LS (60 minutes after FDG injection) is appropriate for demonstrating decreased regional glucose metabolism in patients with AD.

Conclusion

Our study showed that LS during FDG PET is superior to ES in detecting the wide hypometabolic regions of patients with AD. In FDG PET examination of patients with AD, emission scanning soon after the administration of FDG is probably not advised.

References

1. Kumar A, Braun A, Schapiro M, Grady C, Carson R, Herscovitch P. Cerebral glucose metabolic rates after 30 and 45 minute acquisitions: A comparative study. *J Nucl Med* 1992;33: 2103-2105
2. Ishii K, Sasaki M, Kitagaki H, et al. Reduction of cerebellar glucose metabolism in advanced Alzheimer's disease. *J Nucl Med* 1997;38:925-928
3. Iida H, Miura S, Kanno I, et al. Design of evaluation of Headtome IV: a whole body positron emission tomograph. *IEEE Trans Nucl Sci* 1989;37:1006-1010
4. Ishii K, Willoch F, Minoshima S, et al. Statistical brain mapping of ^{18}F -FDG PET in Alzheimer's disease: validation of anatomic standardization for atrophied brains. *J Nucl Med* 2001;42: 548-557
5. Minoshima S, Frey KA, Koeppe RA, Foster NL, Kuhl DE. A diagnostic approach in Alzheimer's disease using three-dimensional stereotactic surface projections of fluorine-18-FDG PET. *J Nucl Med* 1995;36:1238-1248
6. Friston KJ, Holmes AP, Worsely KJ, Poline JB, Frith CD, Frackowiak RSJ. Statistical parametric maps in functional imaging: a general linear approach. *Hum Brain Map* 1995;2:189-210
7. Schmidt K, Lucignani G, Moresco RM, et al. Errors introduced by tissue heterogeneity in estimation of local cerebral glucose utilization with current kinetic models of the [^{18}F]fluorodeoxyglucose method. *J Cereb Blood Flow Metab* 1992;12:823-834
8. Ishii K, Sakamoto S, Hosaka K, Mori T, Sasaki M. Variation in FDG uptake in different regions in normal human brain as a function of the time (30 and 60 minutes) after injection of FDG. *Ann Nucl Med* 2002;16:299-301
9. Fukuyama H, Kameyama M, Harada K, et al. Glucose metabolism and rate constants in Alzheimer's disease examined with dynamic positron emission tomography scan. *Acta Neurol Scand* 1989;80:307-313
10. Minoshima S, Foster NL, Kuhl DE. Posterior cingulate cortex in Alzheimer's disease. *Lancet* 1994;344:895
11. Turkington TG, Coleman RE, Schubert SF, et al. An evaluation of post-injection transmission measurement in PET. *IEEE Trans Nucl Sci* 1993;41:1538-1544